SCIENCE CHINA
Chemistry

• MINI REVIEWS •

February 2018 Vol.61 No.2: 143–152
https://doi.org/10.1007/s11426-017-9162-3

# Assemblies of covalent organic framework microcrystals: multiple-dimensional manipulation for enhanced applications

Fuyu Yuan, Jing Tan & Jia Guo*

*State Key Laboratory of Molecular Engineering of Polymers, and Department of Macromolecular Science, Fudan University, Shanghai 200433, China*

Received July 21, 2017; accepted October 26, 2017; published online January 5, 2018

Covalent organic frameworks (COFs) are well known as the next generation of shape-persistent zeolite analogues, which have brought new impetus to the development of porous organic materials as well as two-dimensional polymers. Since the advent of COFs in 2005, many striking findings have definitely proven their great potentials expanding applications across energy, environment and healthcare fields. With thorough exploration over a decade, research interest has been drawn on the scientific challenges on chemistry, while making full play of COF values has remained far from satisfactory yet. Thus opening an avenue to modulating COF assemblies on the multi-scale is no longer just an option, but a necessity for matching the application requirements with enhanced performances. In this mini-review, we summarize the recent progress on design of nanoscale COFs with varying forms. Detailed description is concentrated on the synthetic strategies of COF assemblies such as spheres, fibers, tubes, coatings and films, thereby shedding light on the flexible manipulation over dimensions, compositions and morphologies. Meanwhile, the advanced applications of nanoscale COFs have been discussed here with comparison of their bulky counterparts.

**covalent organic frameworks, controllable synthesis, porous materials, nanoscale**

**Citation:** Yuan F, Tan J, Guo J. Assemblies of covalent organic framework microcrystals: multiple-dimensional manipulation for enhanced applications. *Sci China Chem*, 2018, 61: 143–152, https://doi.org/10.1007/s11426-017-9162-3

## 1 Introduction

In addition to the well-known zeolites that are naturally formed porous materials, significant progress has been achieved in the artificial construction of micro/meso-pores in functional polymers. Of varying members, covalent organic frameworks (COFs), have attracted increasing attention as they are deemed a next generation of shape-persistent zeolite analogues [1]. Such organic materials constitute a family of crystalline porous polymers, which are featured with designable ordering structures, periodic pore channels, and adaptable chemical functionalization, having thus been responsible for fantastic potentials in light harvesting/emission [2,3], sensing [4], semiconducting [5], photocatalysis [6], proton conductivity [7,8], charge storage [9], and the like in the environmental and energy fields. Also, different synthetic strategies of COFs have well been documented with the aim of development of versatile topological structures [10–16], reaction types [17–22] and functional modules [23–31]. Although the COF-related researches have blossomed to what it is today, the main challenges have remained on their utilization because the performances of powdered COFs have often been not satisfactory if without fine control over the sizes and shapes as well as surface natures of COFs [32]. The tremendous attempts have been devoted to manage the oriented and confined growth of COF microcrystals into uniform and specific nanomaterials such as nanospheres, nanofibers, nanosheets, and free-standing films. Up to date, there has been lasting progress achieved on the dimensional

*Corresponding author (email: guojia@fudan.edu.cn)

manipulation of COFs benefiting their extended utilizations of beyond the conventional fields as well as improved performances.

In this mini-review, we implement a survey for generally covering the substantial progress in recent years on the theme of nanoscale COFs (NCOFs) with varying forms. Note that summaries on design principles, synthetic chemistry, and characterizations of COFs would not be discussed because this part has been systematically described in the past reviews [33]. Also, to focus on the specific topic, two-dimensional polymers with a single-layer structure on substrates are beyond the scope of this review on account of their structural characters without typical COF stacking and periodic pore channels [34].

## 2 Colloidal NCOFs

Miniaturization of bulky COFs in three dimensions with improved solution properties is of significance to promote their performances in sophisticated systems. Pioneering studies on application of COF colloids have recently commenced on the biomedical fields, such as bio-imaging, drug delivery, phototherapy and anti-bacteria. To adapt the physiological conditions, they have been equipped with multiple functions and modified for the usage effectiveness. However, preparation of COF nanospheres having both uniformity and crystallinity remains largely challenged yet; only a few publications have reported on this line thus so far. Zhao and co-workers [35] incorporated triptycene into the vertices of boronate ester-linked COFs in order to attenuate π-π interaction between neighboring layers. Besides the few-layer nanosheets observed, hollow nanospheres coexisted in the products. The feeding concentrations of monomers decided the relative amounts of nanosheets and nanospheres formed in the reaction. The nanospheres were the major product at increased concentrations and grew up to micrometer level with prolonging reaction time. The morphology and size of the nanospheres were quite uniform, displaying a 200-nm diameter and a hollow cavity with the mono- or few-layer-shell thickness, but the long-range ordering structure was absent within the COF nanospheres. The maximum BET surface areas reached as high as 973 $m^2/g$ due to the formation of the amorphous covalent frameworks.

Then an important progress has been achieved by Banjener group [32] with the aim of improvement of the crystallinity of COF nanomaterials. They addressed a template-free method to synthesize COF microcapsules by the Schiff-base reaction of 1,3,5-tris(4-aminophenyl)benzene (Tab) and 2,5-dihydroxyterephthalaldehyde (Dha) under solvothermal conditions (Figure 1(a)). The obtained COFs displayed the hollow structure with a broad size distribution from 0.5 to 4 μm. In contrast to Zhao's results [35], the high crystallinity of COFs remained in the microcapsules because the intramolecular hydrogen bonding between hydroxyl and imine groups enhanced structural rigidity and planarity of the frameworks for oriented stacking. Additionally, it was found that the initially formed morphology was rod-like, which could be assembled into different shapes such as nanorods and solid particles. Afterwards, the assemblies were slowly transformed into a hollow sphere by an inside-out Ostwald ripening (Figure 1(b)). The systematic studies indicated that the formation of such hollow shapes was dependent on the reaction conditions including solvent species and reaction temperatures, and the used method was adapted to some of the other reported imine-linked COFs. Subsequently, they varied the molecular conformations of building blocks for modulating the morphologies of COFs [36]. The two nanostructures, hollow sphere and ribbon, were observed, when the designed frameworks were composed of the hexagonal macrocycles with phenyl- or triazine-centered vertices, respectively. In combination with the theoretical calculations, π-π stacking interaction between the neighboring layers was proved influential to the formed morphologies as well as the surface areas. Compared with the phenyl-core structures, the triazine units were more coplanar with the three phenyl rings connected around the center. This leads to the favorable stacking of adjacent COF layers and a large extension along the *Z* direction to form a nanoribbon. In the other case, the hollow spheres were obtained as a result of a morphological evolution controlled by an inside-out Ostwald ripening.

As reported early, we found that the high qualities both in crystallinity and colloidal properties were difficultly achieved at the same time by using the typical solvothermal system. To circumvent the issue, we proposed a disorder-to-order interconversion strategy for controlled synthesis of COF-based microspheres [37]. The process occurred on the pre-designed microspheres that were formed by a seed-controlled precipitation polymerization, resulting in a uniform nanostructure with $Fe_3O_4$ nanocluster in core and amorphous polyimine network in shell. Depending on the reversible imine exchange, the polyimine shells were transformed into imine-linked COF shell by the direct solvothermal treatment of microspheres without change of the whole colloidal size, shape and structure (Figure 2). This method also could flexibly tune the thickness of COF shell and was adaptive to different building blocks as well. The photothermal conversion on COF shell was firstly reported to demonstrate the potential capability of imine-COFs for phototherapy applications. After that, Wang and co-workers [38] found that imine-linked COFs could form an continuous shell on the surface of $NH_2$-modified silica microspheres by one-step solvothermal method. Subsequent etching of silica cores generated a hollow COF spheres. The morphology of COF shells with different thicknesses were well remained, but the crystallinity of COFs compromised to some extent likely due to the acid-etching damage of the COF structure.

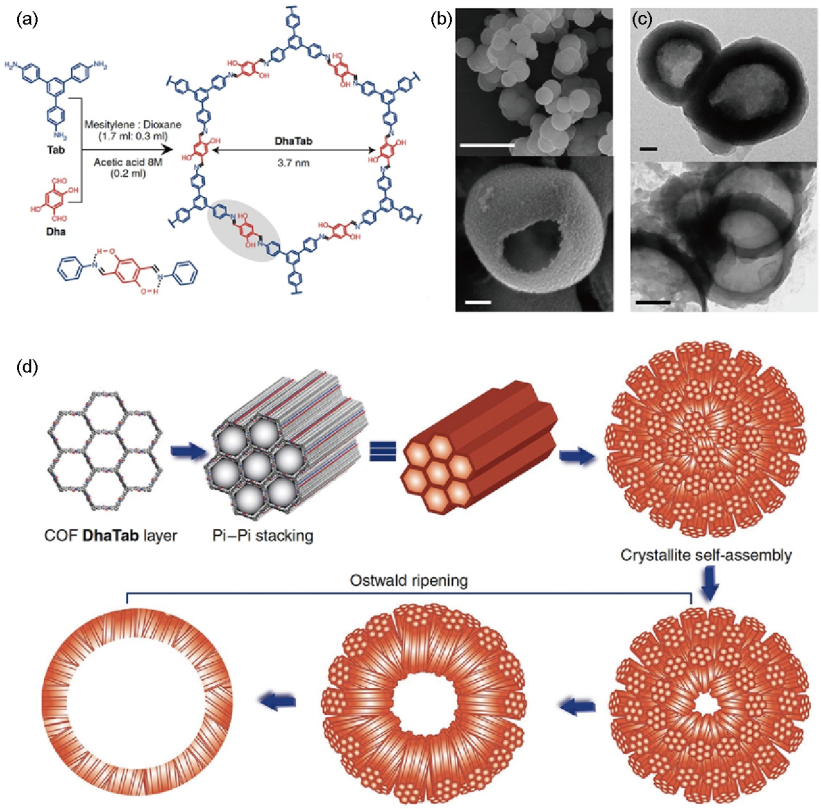


**Figure 1** (a) Synthesis of COF-DhaTab by the Schiff base reaction of Tab and Dha; (b, c) scanning electron microscope (SEM) (b) and transmission electron microscope (TEM) (c) images of COF-DhaTab hollow microspheres; (d) proposed mechanism of the formation of COF hollow spheres [32] (color online).

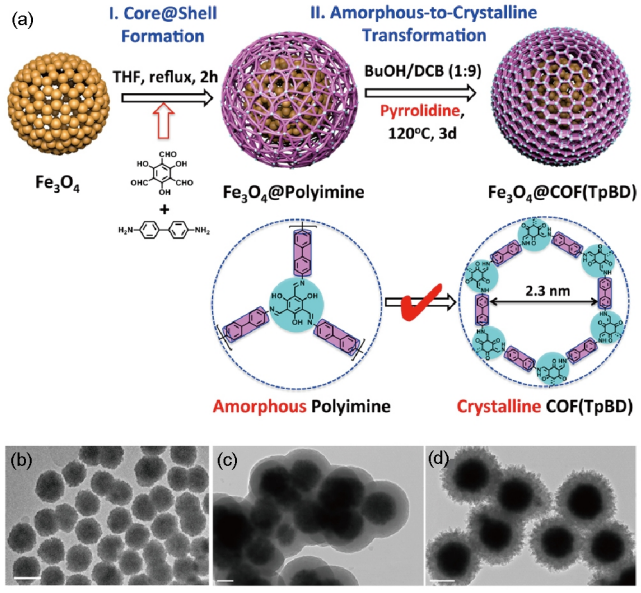


**Figure 2** (a) Schematic representation of preparing imine-linked COF composite microspheres through the amorphous-to-crystalline conversion process; (b–d) TEM images of $Fe_3O_4$ nanoclusters (b), $Fe_3O_4$@Polyimine (c), and $Fe_3O_4$@imine-COF (d) [37] (color online).

Aside from the imine-based COFs, Dichtel *et al.* [39] adopted a homogenous polymerization to fabricate the colloidal COFs with the linkage of boronate ester groups. In addition to the reaction solvents (dioxane/mesitylene), the co-solvent acetonitrile ($CH_3CN$) of different volume fractions could inhibit the aggregation of COF microcrystals to make the colloidal dispersion stand for weeks. This nitrile-assisted method was available to the different kinds of boronate ester-linked COFs because the attractive forces among microcrystals were attenuated by the interaction of boronate linkages with $CH_3CN$. Also, varying the concentrations of co-solvent $CH_3CN$ could control the colloidal sizes, morphologies and surface natures. Solution casting of such colloids yielded a free-standing transparent COF film with retained crystallinity and porosity as well as preferential orientation.

The inorganic/organic hybrid particles have been explored for spanning applications of the COF nanomaterials. Li *et al.* [40] doped $Pd^{2+}$ ions within the coordination sites on an imine-linked COF microcapsule. After the high-temperature carbonization, the immobilized Pd ions were reduced to the nanocrystals, accompanied with the conversion of COF skeletons into N-doped carbon materials. The newly formed hybrids showed the enhanced catalytic activity and selectivity in the hydrogenation of nitrobenzene in ethanol and oxidation of cinnamyl alcohol compared with the commercial Pd/C catalysts. Lu *et al.* [41] reported a

simple method of encapsulating Au nanoparticles within the COF microspheres. In contrast to the early reports, the mild conditions (at 70 °C for 24 h in a flask) were applied for the reaction of 1,3,5-tris(4-aminophenyl)-benzene and 2,5-dimethoxyterephthaldehyde in the presence of PVP-stabilized Au nanoparticles. The formed product had very uniform spherical morphology and entrapped the Au nanoparticles in the central region, leading to a well-defined core/shell nanostructure. Gascon *et al.* [42] proposed a phase inversion method to prepare the COF-based beads with incorporated organometallic complexes. Polyimide was used as a binder (Matrimid 5218) to suspend COF powders in solution, and the composite particles encapsulating Ir was formed by pumping the above mixture to water with a microfluidic device. The prepared beads with accessible porosity and high mechanical stability could be used as catalysts for the direct hydrogenation of $CO_2$ into formic acid under mild conditions.

## 3 One-dimensional NCOFs

Similar to the COF colloids, oriented growth or construction of one-dimensional COF assemblies has not been explored very much. Banerjee and co-workers [43] reported a template-mediated synthesis of hollow tubular COFs using a two-step strategy. ZnO nanorods were wrapped with COF layers by a typical Schiff-base reaction of 1,3,5-triformylphloroglucinol and *p*-phenylenediamine. Then the inside templates were etched by acid (1 M HCl) to leave the hollow nanostructures in quantitative yield (Figure 3). The COF shell was clearly observed without collapse or decomposition, and also, the chemical compositions as well as crystallinity and porosity of COFs retained intact, as a result of the high tolerance of COFs to acid treatment. By the similar strategy, Wang *et al.* [44] proposed an interfacial polymerization approach to encapsulation of imine-linked COFs on the $NH_2$-modified 1D carbon nanotubes. The results emphasized that the appropriate surface modification of the templates was necessary to achieve the controllable shell properties and enhanced crystallinity of COF-based composites.

Dichtel *et al.* [45] developed a template-free method for control over 1D morphologies of COF nanomaterials. The precursor 2,3,6,7,10,11-hexahydroxytriphenylene was installed with aliphatic side chains to remain only two reactive sites for condensation with boronate linkers. As a result, the extension of periodic COFs was impeded to obtain the discrete hexagonal macrocycles (Figure 4(a, b)). Through the self-assembly of those macrocycles, the nanorods were formed to show a high aspect ratio with uniform widths of 2.6 nm and lengths ranging from 100 to 500 nm (Figure 4(c)). The long-range ordering of the nanotubes, which was comparable to that of 2D COFs, followed the arrangement of cofacially stacking macrocycles, but without showing porous structure. The introduced aliphatic side chains provided the additional solubility in solvents such as NMP and DMF, wherein the resulting assemblies were more dynamic. The nanotubes could be disrupted by sonication and spontaneously reformed after 12 h of free standing.

Several other examples have also been reported to give 1D morphologies while growing COFs in solvothermal systems. Jiang group [5] obtained the short nanobelts from the synthesis of boronate ester-linked COFs with pyrene and triphenylene units positioned on the edges and vertices of hexagonal frameworks, respectively. Salonen and co-workers [46] applied the molecular dipole interaction of pyrene dione and triphenylene to control the evolution of rod-like COFs. Liu *et al.* [47] proposed a vapor-assisted grinding approach to improving the aldehyde-amine condensation, in which the nanofibers was transformed from the initial COF grains. They profiled the morphological conversion to a dissolution-

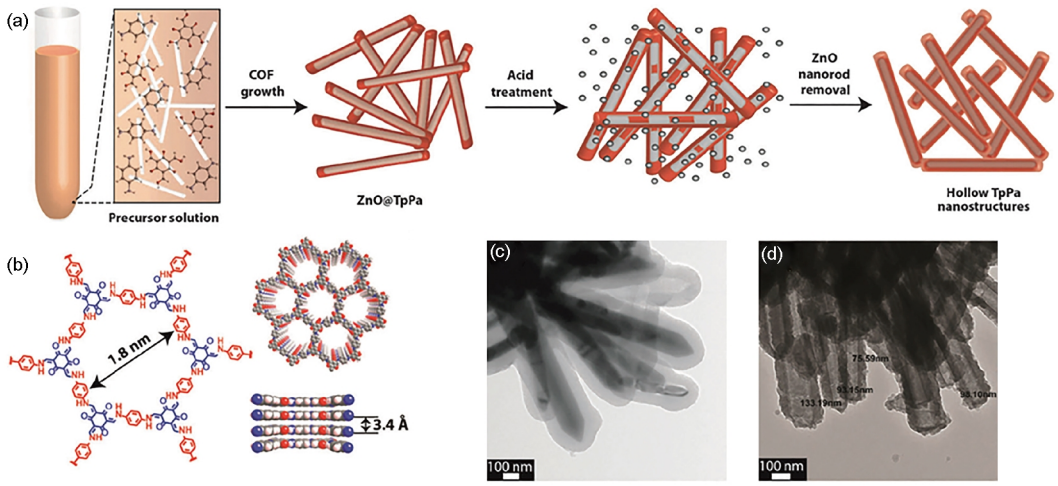


**Figure 3** (a, b) Synthesis of highly stable and hollow COF nanotubes via a template-mediated strategy, and (c, d) TEM images of ZnO@COF (c) and COF nanotubes (d) [43] (color online).

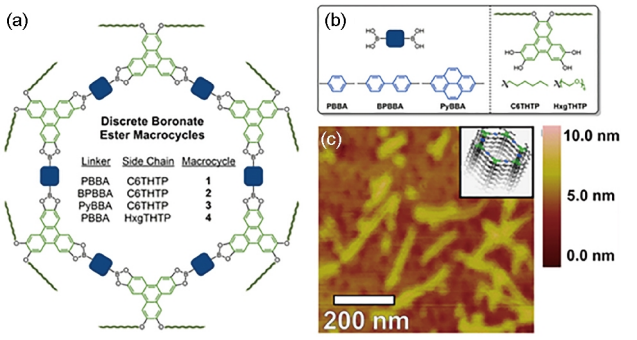


**Figure 4** (a, b) Schematic analogues of discrete boronate-ester macrocycles (a) prepared by the differernt precursors (b); (c) atomic force microscope (AFM) image of the nanotubes assembled by the designed macrocycles [45] (color online).

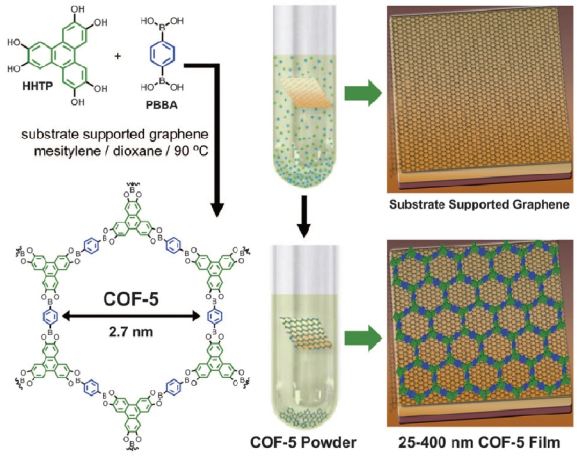


**Figure 5** Solvothermal condensation of HHTP and PBBA on the surface of a substrate-supported SLG to form a continuous COF-5 film [49] (color online).

recrystallization process. Meanwhile, a microfluidic technique was applied to finely modulate the flow ratios of monomers and catalysts, being able to obtain a macroporous sponge with interpenetrated COF nanofibers that reserved the microporosity and crystallinity [48].

## 4 Two-dimensional NCOFs

### 4.1 Substrate-supported thin films

Researchers have devoted great deal of enthusiasm to synthesis of 2D organic polymers over decades. In the view of the 2D structural characters reported on COFs, there are two distinct strategies developed for the COF-based 2D polymers, namely bottom-up synthesis and top-down delamination. The first example was reported by Dichtel group [49] (Figure 5), who solvothermally prepared an oriented COF coating on a surface of single-layer graphene (SLG) supported with different substrates including Cu, $SiO_2$ and SiC. The formed COF layer had nearly no grains on the surface, appeared fibrous in texture, and showed the area of over ~100 $\mu m^2$ with uniform thickness that can be controlled from ca. 70 to 200 nm. The crystallinity and alignment of COF coatings on the substrate were evidenced for the possibility to explore new electronic devices on basis of the potential oriented π-electron mobility, but the given pores were too small to accommodate complementary semiconductors. Thus their group addressed the expansion of pore widths by varying the edge lengths on the phthalocyanine-based tetragonal frameworks [50]. All of these powdered COFs had superior crystallinity, and the expected pore sizes were tuned from 2.7 to 4.4 nm. The corresponding oriented films covered on a transparent SLG-modified silica substrate were characterized by grazing incidence X-ray diffraction, showing the typical COF structures and vertical alignment with respect to the substrates. The thickness of the films achieved was up to several hundreds nanometers, depending on the properties of bi-aldehyde linkers. In light of the above structural features of oriented COF films, Dichtel group [51] assembled the redox-active COFs into supercapacitors for energy storage. The reversible redox property of the synthesized COFs was due largely to the incorporation of 2,6-diaminoanthraquinone into the frameworks. Following the same route, the oriented COF coatings of 200-nm thickness were yielded on the surface of Au substrate for being electrodes of supercapacitors. The areal capacitances reached as high as 3.0 mF/$cm^2$, because a large fraction of the redox-active anthraquinone moieties was able to access the electrodes. As control, the insoluble COF powders led to the poor contact of redox-active compositions with the electrodes, thus giving a moderate capacitance (~0.4 mF/$cm^2$). Unambiguously, the crystalline and oriented COF coatings would become attractive candidates as active matters to develop organic electronics.

Along this line, Bein and co-workers [52] synthesized a uniform, oriented and crystalline COF film on an ITO-coated glass, displaying a thickness of about 150 nm and a mesopore structure (Figure 6). As observed, the film growth tended to follow an island-fused pathway. Since benzodithophene (BDT) was incorporated into COF skeletons, the fullerene derivatives [60]PCBM and [70]PCBM were entrapped in BDT-COF films to study the electron transfer capabilities. Roughly 60% fluorescence of BDT-COF was quenched, and a longer decay time was detected from transient absorption measurement, indicative of the electron injection from the COF donors to the PCBM acceptors and further formation of polarons at the donor/acceptor interface. They subsequently adopted the same BDT-COF film to construct a hole-only device with the architecture of glass/ITO/$MoO_x$/BDT-COF/$MoO_x$/Au. The thickness-dependent hole mobility was measured in the dark in the range from $3\times10^{-7}$ to $6\times10^{-9}$ $cm^2$/V s; the thinner films were responsible for the highest values. This trend implies the

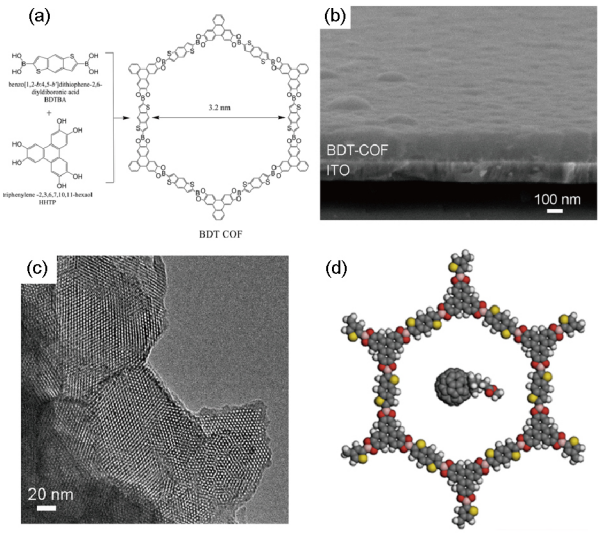


**Figure 6** (a) Synthesis of boronate-ester linked BDT-COF; (b, c) SEM (b) and TEM (c) images of BDT-COF thin film grown on an ITO-coated glass and a gold surface, respectively; (d) entrapment of fullerene molecules within pore channels of BDT-COF [52] (color online).

presence of transport barriers due to the COF stacking defects. Upon illumination of white light LED, a 3-fold increase of the mobility was tested, demonstrating its photoactive property. Additionally, the exceptionally low dielectric constant was found to be around 1.7 as a result of the formed COF film with low density and highly porous structure.

Liu *et al*. [53] reported another electroactive COF based on tetrathiafulvalene (TTF) that is a well-known electron donor with high charge-transfer conductivity. The thin film of TTF-COF with uniform thickness of around 150 nm was grown on $Si/SiO_2$ substrates and transparent ITO-coated glass, respectively, by the Schiff-base reaction in the solvothermal system. Once the obtained TTF-COF film was doped with $I_2$ or TCNQ, the TTF radical cations were largely generated to favor the conductivity, reaching a maximum of 0.28 S/m. Also, the mixed valence TTF, which was formed between TTF and TTF radical cations, allowed for the delocalization of free radicals across the vertically stacking sheets. This is a consequence of the relatively high conductivity as well as red-shift absorption in the oriented TTF-COF films. Inspired with the early findings, Wang *et al*. [54] reported the synthesis of single-layer TTF-COFs on the highly ordered pyrolytic graphite (HOPG) substrate, and proved the preferential orientation of COF layers in alignment with HOPG lattices. Also, they suggested that the decrease of the TTF-COFs' lattice sizes could facilitate the formation of large-scale ordering layers with its structural regularity. Then they addressed an precise control of the formed number of TTF-COF layers by tuning the feeding amount of TTF units [55]. A direct evidence given by high resolution scanning tunneling microscopy has validated that a double-layer TTF-COF was formed on the HOPG substrate, wherein the lower COF layers were continuously covered onto the whole HOPG surface and the upper COFs extended discretely over the lower layer.

Although the solution-phase fabrication of COF films on substrates has been proved effective, the approach has limitations on control of the film formation. The COF precipitates would contaminate the film, and the film thickness was hard to be accurately tuned. Dichtel *et al*. [56] utilized a flow cell to prepare boronate ester-linked COF films in order to avoid contamination and precisely adjust film thickness (Figure 7). A homogenous solution at the initial time must be required to provide an induction period for the flow running. The reaction mixture was pumped through a reservoir at designed temperatures and into a flow cell equipped with a quartz crystal microbalance substrate for monitoring mass changes. The residence time ($t_r$), which was the period before monomers arrived at substrate, played a vital role in the film deposition and crystallinity. A shorter $t_r$ caused a slow growth of films with amorphous structures. While $t_r$ was longer, the COF films were rapidly formed and showed good crystallinity. A series of 2D hexagonal COF films were prepared by the method, indicative of its generality. The observation of film texture revealed the smooth surface with less contaminates, and the growth of COF films in flow could make control of film thickness, which is much larger than those prepared by the conventional systems.

To circumvent the scalability of COF films, Bein *et al*. [57] presented a concept of vapor-assisted conversion for the scale-up synthesis of boronate ester-linked COFs. Typically, the precursor solution was drop-cast on glass substrate, and it was immediately placed into a desiccator with a small vessel containing mesitylene and dioxane at a given volume ratio. While storing for 72 h at room temperature, a continuous and smooth layer of COFs was formed by the inter-growing of particles on the glass. The film thickness could be easily controlled from a few hundred nanometers to several microns by varying the concentrations of precursor solutions.

### 4.2 Covalent organic nanosheets

Top-down delamination of COFs is another important strategy to obtain 2D macromolecular nanosheets from COFs because the layered structures are maintained only by the relatively weak Van der Waals forces. Zamora *et al*. [58] reported the delamination of boronate ester-linked COFs to produce thin layered nanosheets by using the sonication under suitable conditions. Dichloromethane was the most effective solvent for COF-8 synthesized by the condensation of 2,3,6,7,10,11-hexahydroxytriphenylene and 1,3,5-tris[4-phenylboronic acid]benzene. After 15-min sonication (frequency: 24 kHz; amplitude: 42 μm), the exfoliated nanosheets of COF-8 comprised 10–25 layers with reproducible heights of 4–10 nm and lateral dimensions of several micrometers. Dichtel and co-workers [59] further

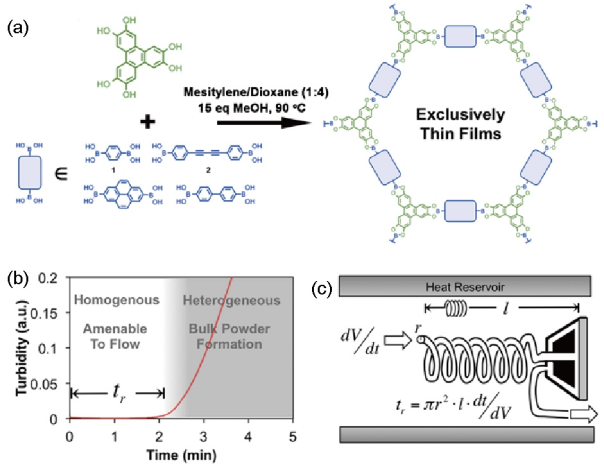


**Figure 7** (a) Illustration of boronate ester-linked COFs for preparation of thin films; (b) turbidity as a function of reaction time during the formation of COF; (c) schematic of flow setup designed with variable induction periods [56] (color online).

demonstrated that some other laboratory solvents such as water, dioxane and DMF could exfoliate and disperse a 2D hydrazine-linked COF (COF-43). As treated with dioxane, the solvated COF-43 nanosheets retained long-range hexagonal ordering and displayed high aspect ratios with lateral widths of 200 nm and average heights of 1.32±0.37 nm. Banerjee *et al.* [60] also successfully exfoliated COFs with isopropyl alcohol at room temperature. The obtained nanosheets showed the enhanced fluorescence as well as a blue shift in spectra with respect to their bulk counterparts. Such nanosheets could optically detect nitroaromatic compounds, showing high selectivity toward 2,4,6-trinitrophenol (TNP) which led to 63% quenching efficiency at its concentration of $5.4\times10^{-5}$ M. Interestingly, when the nanosheets were coated on a paper strip for the solid-state detection, the 10-fold enhanced fluorescence as well as a distinct color change was observed once the TNP solution was deposited on. This indicated the superior "turn-on" detection for TNP in the solid state.

Since mechanochemistry could help make many chemical processes more environmentally and friendly in industry, this technology has thus been tried in the laboratory for the scalable synthesis of COFs. Banerjee group [61,62] reported a solvent-free grinding method to proceed the Schiff-base reaction of 1,3,5-triformylphloroglucinol and different diamine compounds. They found those COF products with nanosheet-like structures (Figure 8). The typical appearance seemed like the very thin graphite with lateral dimensions of several micrometers and thickness of 3–10 nm, corresponding to that of 10–30 COF layers. It indicated that the used mechanical force was strong enough to delaminate the multilayers of imine-linked COFs, while remaining the structural integrity as well as 2D motifs. The surface areas decreased dramatically, but the crystallinity of exfoliated nanosheets remained to some extent, displaying a decrease of the first peak (100 plane) and the broadening of the last peak (001 plane). This implies the random displacement of the 2D layers with each other and largely compromised the surface areas of such materials. The mechanical grinding is a scalable and energy efficient method as compared to the other existing methods such as sonication, CVD and interfacial growth *in situ*. Feng *et al.* [63] applied a balling mill technique to delaminate redox-active COFs into few-layer nanosheets used as cathode materials of lithium-ion batteries. The exfoliated COFs could shorten the ion/electron migration length to benefit their diffusion in comparison with the bulky COFs. It was impressive that the anthraquinone-based nanosheets rendered as high as 96% of theoretical capacity at 20 mA/g and were stable at a capacity of 104 mA h/g over 1800 cycles (500 mA/g).

Functionalization of COFs with reactive groups provides an innovative way to exfoliate multilayer structures during the COF formation. Banerjee *et al.* [64] synthesized an ionic nanosheet originated from the COFs positively charged with guanidinium units. They further studied the antibacterial performances of ionic nanosheets and proved that the electrostatic interactions between positively charged frameworks and negatively charged phospholipid bilayer of bacterial membranes could result in good activity against both Gram-positive and Gram-negative bacteria. Another example reported by Banerjee group [65] was the post functionalization of anthracene-based COFs with *N*-hexylmaleimide by a Diels-Alder cycloaddition pathway. The large substituents caused the loss of π-π stacking to disassemble COF layers into nanosheets. Then a thin film was cast at the air/water interface by piling up the nanosheets to give a uniform thickness of several nanometers (Figure 9). Bottom-up synthesis of COF nanosheets has been simultaneously developed. Zhang *et al.* [66] synthesized a monolayer imine-linked nanosheet at the air/water interface by incorporating three *n*-hexyl groups on the vertices of COF frameworks. Amphiphilic property of the frameworks ensured the interfacial growth of a monolayer nanosheet. Although the molecular structures were difficulty defined, the formation of such smooth, coherent, large and free-standing polyimine monolayers was evidenced substantially.

## 5 Conclusions

In this short review, we have described the recent progress of COF nanomaterials both in synthesis and applications. Inspired by the concept of bottom-up design, template-mediated methodology is general and flexible to make COFs have the versatile forms such as core/shell microspheres, hollow microcapsules, nanotubes, coatings and films. Also, the incorporation of template materials such as $Fe_3O_4$, ZnO, ITO, and graphene improves the utilization performances of COFs as these hybrids could be directly used for energy devices, as well as for the other innovative applications such as

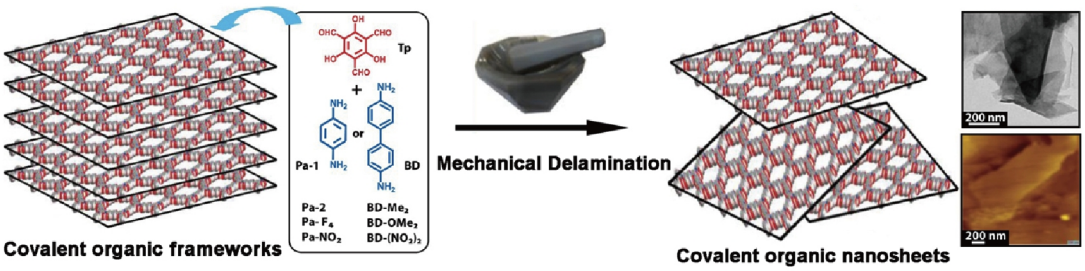


**Figure 8** Illustration of mechanical delamination of imine-linked COFs toward discrete nanosheets [62] (color online).

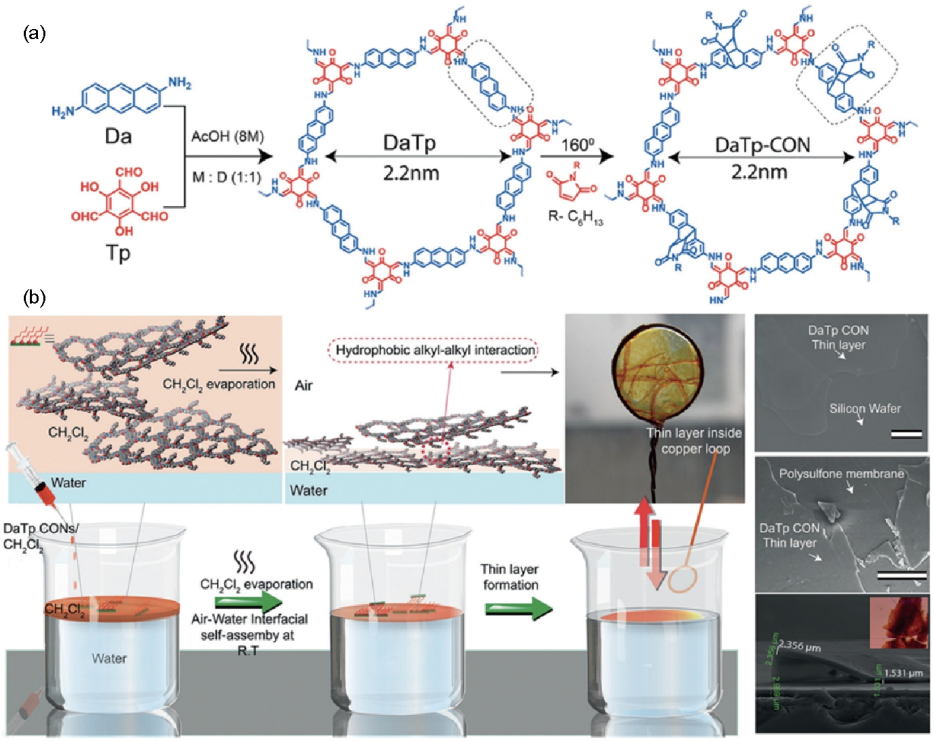


**Figure 9** (a) Synthetic procedure of DaTp-COF and DaTp-CON; (b) casting of a scalable thin film of DaTp-CONs by the method of air/water interfacial assembly [65] (color online).

biomedical fields. On the other hand, top-down strategy has been developed to disassemble COFs to discrete colloids or nanosheets dispersed in solution. This is mainly attributed to the weak π-π interaction among adjacent layers, thus allowing for the delamination of COFs by solvation, sonication, and grinding under mild conditions. Also, dangling substituents on the organic frameworks endow COFs with hydrophilic, hydrophobic or ionic properties for the ease of delamination. Since the bulky COFs are neither kind of single crystals nor assembled to regular aggregates, they are difficult to realize the full value of COFs in utilizations. Therefore, the controlled assemblies of COF microcrystals with intended sizes, morphologies and dimensions would create opportunities to access the versatile applicability and circumvent the limitations of bulky COFs for largely improving their performances.

**Acknowledgments** This work was supported by the National Natural Science Foundation of China (21474015, 21774023), and Science and Technology Commission of Shanghai Municipality (14ZR1402300).

**Conflict of interest** The authors declare that they have no conflict of interest.

1 Mastalerz M. *Angew Chem Int Ed*, 2008, 47: 445–447
2 Nagai A, Chen X, Feng X, Ding X, Guo Z, Jiang D. *Angew Chem Int Ed*, 2013, 52: 3770–3774
3 Dalapati S, Jin E, Addicoat M, Heine T, Jiang D. *J Am Chem Soc*, 2016, 138: 5797–5800
4 Dalapati S, Jin S, Gao J, Xu Y, Nagai A, Jiang D. *J Am Chem Soc*, 2013, 135: 17310–17313
5 Wan S, Guo J, Kim J, Ihee H, Jiang D. *Angew Chem*, 2008, 120: 8958–8962
6 Vyas VS, Haase F, Stegbauer L, Savasci G, Podjaski F, Ochsenfeld C, Lotsch BV. *Nat Commun*, 2015, 6: 8508

7 Chandra S, Kundu T, Kandambeth S, Babarao R, Marathe Y, Kunjir SM, Banerjee R. *J Am Chem Soc*, 2014, 136: 6570–6573
8 Ma H, Liu B, Li B, Zhang L, Li YG, Tan HQ, Zang HY, Zhu G. *J Am Chem Soc*, 2016, 138: 5897–5903
9 Mulzer CR, Shen L, Bisbey RP, McKone JR, Zhang N, Abruña HD, Dichtel WR. *ACS Cent Sci*, 2016, 2: 667–673
10 Côté AP, El-Kaderi HM, Furukawa H, Hunt JR, Yaghi OM. *J Am Chem Soc*, 2007, 129: 12914–12915
11 El-Kaderi HM, Hunt JR, Mendoza-Cortes JL, Cote AP, Taylor RE, O'Keeffe M, Yaghi OM. *Science*, 2007, 316: 268–272
12 Cai SL, Zhang K, Tan JB, Wang S, Zheng SR, Fan J, Yu Y, Zhang WG, Liu Y. *ACS Macro Lett*, 2016, 5: 1348–1352
13 Liu Y, Ma Y, Zhao Y, Sun X, Gándara F, Furukawa H, Liu Z, Zhu H, Zhu C, Suenaga K, Oleynikov P, Alshammari AS, Zhang X, Terasaki O, Yaghi OM. *Science*, 2016, 351: 365–369
14 Pang ZF, Xu SQ, Zhou TY, Liang RR, Zhan TG, Zhao X. *J Am Chem Soc*, 2016, 138: 4710–4713
15 Lin G, Ding H, Chen R, Peng Z, Wang B, Wang C. *J Am Chem Soc*, 2017, 139: 8705–8709
16 Qian C, Qi QY, Jiang GF, Cui FZ, Tian Y, Zhao X. *J Am Chem Soc*, 2017, 139: 6736–6743
17 Côté AP, Benin AI, Ockwig NW, O'Keeffe M, Matzger AJ, Yaghi OM. *Science*, 2005, 310: 1166–1170
18 Kuhn P, Antonietti M, Thomas A. *Angew Chem Int Ed*, 2008, 47: 3450–3453
19 Uribe-Romo FJ, Hunt JR, Furukawa H, Klöck C, O'Keeffe M, Yaghi OM. *J Am Chem Soc*, 2009, 131: 4570–4571
20 Uribe-Romo FJ, Doonan CJ, Furukawa H, Oisaki K, Yaghi OM. *J Am Chem Soc*, 2011, 133: 11478–11481
21 Kandambeth S, Mallick A, Lukose B, Mane MV, Heine T, Banerjee R. *J Am Chem Soc*, 2012, 134: 19524–19527
22 Li H, Pan Q, Ma Y, Guan X, Xue M, Fang Q, Yan Y, Valtchev V, Qiu S. *J Am Chem Soc*, 2016, 138: 14783–14788
23 Wan S, Guo J, Kim J, Ihee H, Jiang D. *Angew Chem Int Ed*, 2009, 48: 5439–5442
24 Ding X, Guo J, Feng X, Honsho Y, Guo J, Seki S, Maitarad P, Saeki A, Nagase S, Jiang D. *Angew Chem Int Ed*, 2011, 50: 1289–1293
25 Wan S, Gándara F, Asano A, Furukawa H, Saeki A, Dey SK, Liao L, Ambrogio MW, Botros YY, Duan X, Seki S, Stoddart JF, Yaghi OM. *Chem Mater*, 2011, 23: 4094–4097
26 Feng X, Chen L, Honsho Y, Saengsawang O, Liu L, Wang L, Saeki A, Irle S, Seki S, Dong Y, Jiang D. *Adv Mater*, 2012, 24: 3026–3031
27 Ding SY, Dong M, Wang YW, Chen YT, Wang HZ, Su CY, Wang W. *J Am Chem Soc*, 2016, 138: 3031–3037
28 Wang X, Han X, Zhang J, Wu X, Liu Y, Cui Y. *J Am Chem Soc*, 2016, 138: 12332–12335
29 Xu HS, Ding SY, An WK, Wu H, Wang W. *J Am Chem Soc*, 2016, 138: 11489–11492
30 Han X, Xia Q, Huang J, Liu Y, Tan C, Cui Y. *J Am Chem Soc*, 2017, 139: 8693–8697
31 Zhang J, Han X, Wu X, Liu Y, Cui Y. *J Am Chem Soc*, 2017, 139: 8277–8285
32 Kandambeth S, Venkatesh V, Shinde DB, Kumari S, Halder A, Verma S, Banerjee R. *Nat Commun*, 2015, 6: 6786
33 Ding SY, Wang W. *Chem Soc Rev*, 2013, 42: 548–568
34 Xu L, Zhou X, Tian WQ, Gao T, Zhang YF, Lei S, Liu ZF. *Angew Chem Int Ed*, 2014, 53: 9564–9568
35 Zhou TY, Lin F, Li ZT, Zhao X. *Macromolecules*, 2013, 46: 7745–7752
36 Halder A, Kandambeth S, Biswal BP, Kaur G, Roy NC, Addicoat M, Salunke JK, Banerjee S, Vanka K, Heine T, Verma S, Banerjee R. *Angew Chem*, 2016, 128: 7937–7941
37 Tan J, Namuangruk S, Kong W, Kungwan N, Guo J, Wang C. *Angew Chem*, 2016, 128: 14185–14190
38 Sun B, Wang D, Wan L. *Sci China Chem*, 2017, 60: 1098–1102
39 Smith BJ, Parent LR, Overholts AC, Beaucage PA, Bisbey RP, Chavez AD, Hwang N, Park C, Evans AM, Gianneschi NC, Dichtel WR. *ACS Cent Sci*, 2017, 3: 58–65
40 Chen L, Zhang L, Chen Z, Liu H, Luque R, Li Y. *Chem Sci*, 2016, 7: 6015–6020
41 Shi X, Yao Y, Xu Y, Liu K, Zhu G, Chi L, Lu G. *ACS Appl Mater Interfaces*, 2017, 9: 7481–7488
42 Bavykina AV, Rozhko E, Goesten MG, Wezendonk T, Seoane B, Kapteijn F, Makkee M, Gascon J. *ChemCatChem*, 2016, 8: 2217–2221
43 Pachfule P, Kandmabeth S, Mallick A, Banerjee R. *Chem Commun*, 2015, 51: 11717–11720
44 Sun B, Liu J, Cao A, Song W, Wang D. *Chem Commun*, 2017, 53: 6303–6306
45 Chavez AD, Smith BJ, Smith MK, Beaucage PA, Northrop BH, Dichtel WR. *Chem Mater*, 2016, 28: 4884–4888
46 Salonen LM, Medina DD, Carbó-Argibay E, Goesten MG, Mafra L, Guldris N, Rotter JM, Stroppa DG, Rodríguez-Abreu C. *Chem Commun*, 2016, 52: 7986–7989
47 Jiang Y, Huang W, Wang J, Wu Q, Wang H, Pan L, Liu X. *J Mater Chem A*, 2014, 2: 8201–8204
48 Rodríguez San Miguel D, Abrishamkar A, Navarro JA, Rodriguez Trujillo R, Amabilino DB, Mas Ballesté R, Zamora F, Puigmartí Luis J. *Chem Commun*, 2016, 52: 9212–9215
49 Colson JW, Woll AR, Mukherjee A, Levendorf MP, Spitler EL, Shields VB, Spencer MG, Park J, Dichtel WR. *Science*, 2011, 332: 228–231
50 Spitler EL, Colson JW, Uribe-Romo FJ, Woll AR, Giovino MR, Saldivar A, Dichtel WR. *Angew Chem Int Ed*, 2012, 51: 2623–2627
51 DeBlase CR, Hernández-Burgos K, Silberstein KE, Rodríguez-Calero GG, Bisbey RP, Abruña HD, Dichtel WR. *ACS Nano*, 2015, 9: 3178–3183
52 Medina DD, Werner V, Auras F, Tautz R, Dogru M, Schuster J, Linke S, Döblinger M, Feldmann J, Knochel P, Bein T. *ACS Nano*, 2014, 8: 4042–4052
53 Cai SL, Zhang YB, Pun AB, He B, Yang J, Toma FM, Sharp ID, Yaghi OM, Fan J, Zheng SR, Zhang WG, Liu Y. *Chem Sci*, 2014, 5: 4693–4700
54 Dong W, Wang L, Ding H, Zhao L, Wang D, Wang C, Wan LJ. *Langmuir*, 2015, 31: 11755–11759
55 Dong WL, Li SY, Yue JY, Wang C, Wang D, Wan LJ. *Phys Chem Chem Phys*, 2016, 18: 17356–17359
56 Bisbey RP, DeBlase CR, Smith BJ, Dichtel WR. *J Am Chem Soc*, 2016, 138: 11433–11436
57 Medina DD, Rotter JM, Hu Y, Dogru M, Werner V, Auras F, Markiewicz JT, Knochel P, Bein T. *J Am Chem Soc*, 2015, 137: 1016–1019
58 Berlanga I, Ruiz-González ML, González-Calbet JM, Fierro JLG, Mas-Ballesté R, Zamora F. *Small*, 2011, 7: 1207–1211
59 Bunck DN, Dichtel WR. *J Am Chem Soc*, 2013, 135: 14952–14955
60 Das G, Biswal BP, Kandambeth S, Venkatesh V, Kaur G, Addicoat M, Heine T, Verma S, Banerjee R. *Chem Sci*, 2015, 6: 3931–3939
61 Biswal BP, Chandra S, Kandambeth S, Lukose B, Heine T, Banerjee R. *J Am Chem Soc*, 2013, 135: 5328–5331
62 Chandra S, Kandambeth S, Biswal BP, Lukose B, Kunjir SM,

Chaudhary M, Babarao R, Heine T, Banerjee R. *J Am Chem Soc*, 2013, 135: 17853–17861
63 Wang S, Wang Q, Shao P, Han Y, Gao X, Ma L, Yuan S, Ma X, Zhou J, Feng X, Wang B. *J Am Chem Soc*, 2017, 139: 4258–4261
64 Mitra S, Kandambeth S, Biswal BP, Khayum M. A, Choudhury CK, Mehta M, Kaur G, Banerjee S, Prabhune A, Verma S, Roy S, Kharul UK, Banerjee R. *J Am Chem Soc*, 2016, 138: 2823–2828
65 Khayum MA, Kandambeth S, Mitra S, Nair SB, Das A, Nagane SS, Mukherjee R, Banerjee R. *Angew Chem Int Ed*, 2016, 55: 15604–15608
66 Dai W, Shao F, Szczerbiński J, McCaffrey R, Zenobi R, Jin Y, Schlüter AD, Zhang W. *Angew Chem Int Ed*, 2016, 55: 213–217